



An electrochemical aptasensing platform for carbohydrate antigen 125 based on the use of flower-like gold nanostructures and target-triggered strand displacement amplification

Jishun Chen¹ · Wanbao Hu² · Jian Wei¹ · Fei Yu¹ · Lun Wu¹ · Ceming Wang¹ · Wei Wang² · Shenyuan Zuo² · Bing Shang¹ · Qinhu Chen^{1,3}

Received: 7 January 2019 / Accepted: 12 May 2019 / Published online: 30 May 2019
© Springer-Verlag GmbH Austria, part of Springer Nature 2019

Abstract

An electrochemical aptasensing method is described for the determination of the biomarker CA125. It combines aptamer recognition and target-triggered strand displacement amplification. Flower like gold nanostructures were electrodeposited on a screen-printed carbon electrode to increase the sensor surface, to assemble more toehold-containing hairpin probe 1 (Hp1), and to improve the accessibility for DNA strands. Under the optimal conditions, this assay has a linear response in the 0.05 to 50 ng·mL⁻¹ CA125 concentration range, with a low detection limit of 5.0 pg·mL⁻¹. This method is specific and stable. It was successfully applied to the detection of CA125 in spiked biological samples, with recoveries between 82.5% and 104.1%.

Keywords Aptasensor · Toehold · Aptamer · Cancer biomarker · Ovarian cancer

Introduction

Ovarian cancer has the highest mortality rate of the three main malignant tumors of the female reproductive system. Most patients are diagnosed in advanced stages due to lack of significant or specific clinical symptoms, which causes a low five-year overall survival rate [1, 2]. Carbohydrate antigen 125 (CA125), a high molecular weight mucin-like glycoprotein,

can promote cancer cell proliferation and inhibit anti-cancer immune responses [1]. Serum levels of CA125 are routinely monitored in patients with ovarian cancer in women (serum threshold level 35 U·mL⁻¹). It has also been considered as a crucial ovarian disease serum-based biomarker to predict the presence of malignancy and the prognosis after treatment [1, 3]. In addition, CA125 has been widely used as one of biomarkers for liver, lung, gastric and breast cancers [4]. Thus, the sensitive detection of CA125 is of great significance for early diagnosis and evaluation of prognosis and therapy effects of cancers.

Immunosensors based on antibody-antigen immune reaction are widely used for carbohydrate antigen detection [5–8]. However, these methods are limited by expensive antibodies and equipments, complicated experimental procedures, long analysis time, as well as the instable substrates. Aptamer based sensors have also been reported to detect CA125 [9, 10]. Compared with antibodies and enzymes, aptamers are easy to synthesize and stable enough to resist harsh environments (pH and temperatures). More importantly, the specific binding of aptamers to target molecules are available for enhancing the detection selectivity [11]. Of note that, the reported quantification biosensors mainly rely on colorimetry [12], electrochemical method [13–19], chemiluminescence [20], electrochemiluminescence [21], plasmon resonance scattering

Jishun Chen and Wanbao Hu are the Co-first authors.

Electronic supplementary material The online version of this article (<https://doi.org/10.1007/s00604-019-3497-3>) contains supplementary material, which is available to authorized users.

✉ Bing Shang
bingshang1126@163.com

✉ Qinhu Chen
cq77@163.com

¹ Affiliated Dongfeng Hospital, Hubei University of Medicine, Shiyan 442008, Hubei, China

² Sinopharm DongfengHuaguo Hospital, Shiyan 442008, Hubei, China

³ Hubei Key Laboratory of Wudang Local Chinese Medicine Research (Hubei University of Medicine), Shiyan 442400, Hubei, China

(PRS) [4], etc.. Among them, electrochemical detection is mostly used owing to its low cost, simple operation and high sensitivity. As for electrodes, screen-printed carbon electrode (SPCE) has given rise to researchers' attention because it is easy to modify, portable, and able to mass production [22]. Nanomaterials have also been used to modify electrode surface to increase the surface areas and the binding performance of biomolecules on the sensing platform [23–25]. In present work, flower like gold nanostructures were electrodeposited on SPCE to increase the biosensing surface for subsequent assembly of more amounts of probes for construction of electrochemical aptasensing platform.

To meet the quantitative requirements of higher sensitivity, biological amplification strategies have been widely used for biosensor construction. The commonly used amplification strategies include strand displacement amplification (SDA) [26], rolling circle amplification (RCA) [27], hybridization chain reaction (HCR) [7] and so on. Among them, SDA exhibits great application prospects due to its isothermal nature, high amplification efficiency, and rapid amplification kinetics [28]. Moreover, the occurrence of SDA can be triggered by targets under mild enzyme-free conditions and reverse low specificity caused by background signals via a relatively simple sequence design [29]. Thus, combination of signal amplification strategy and aptamer recognition will be a promising strategy to realize the higher sensitivity and selectivity of biosensor.

Flower like gold nanostructures were electrodeposited on SPCE to increase the biosensing surface and deflection angles for assembly of more amounts of Hp1 and subsequent accessibility of DNA strands. Based on our previous work [30], combination of target-triggered SDA and aptamer recognition realized the specific and sensitive detection of CA125. In the presence of aptamer/probe A duplex and Hp2 labeled with methylene blue (MB), the introduction of CA125 triggered the 1:N target-signal SDA, leading to more electro active reporter MB in proximity to the modified SPCEs and thus producing higher electrochemical response.

Experimental section

Reagents

Table S1 lists all DNA oligonucleotides that were synthesized and purified by Sangon Biotechnology Co. Ltd. (Shanghai, China; www.sangon.com). Poly(acrylic acid)(PAA), poly(ethylene imine)(PEI), $\text{HAuCl}_4 \cdot 3\text{H}_2\text{O}$ ($\geq 99.9\%$), tris (hydroxymethyl) aminomethane (Tris), tris (2-carboxyethyl) phosphine hydrochloride (TCEP) and 6-mercapto-1-hexanol (MCH) were obtained from Sigma-Aldrich (St. Louis, MO, USA; www.sigmaaldrich.com). CA125, bovine serum albumin (BSA), CD63, epithelial cell adhesion molecule

(EpCAM), and prostate specific antigen (PSA) were obtained from Cusabio Biotech Co. (USA, www.cusabio.com) to verify the specificity of the aptasensing platform for CA125 detection. Other reagents were all of analytical grade. The health human serum, saliva and urine were provided by SinopharmDongfeng General Hospital and approved by the ethical committees of SinopharmDongfeng General Hospital. Ultrapure water was prepared by a Millipore water purification system (18.2 $\text{M}\Omega \cdot \text{cm}$ resistivity, Milli-Q Direct 8) and used in all runs.

Apparatus

Square wave voltammetry (SWV) and chronoamperometry experiments were performed using a CHI660D workstation (CH Instruments Inc., Shanghai, China, <http://www.chinstr.com/>). SWV and chronoamperometry were conducted to detect CA125 and deposit gold nanostructures on SPCE surface, respectively. Screen-printed carbon electrodes (SPCEs) (Delta Biotech, Suzhou, China) comprising a carbon working electrode (diameter: 3 mm), a carbon counter electrode and a silver pseudo reference electrode were utilized. The scanning electron microscopy (SEM, JEOL JSM-6510LV and ZEISS MERLIN Compact) was used to obtain images of surface morphologies of SPCE and SPCE modified with gold nanostructures.

Construction of aptasensing platform

Firstly, SPCEs were sequentially cleaned in ethanol and ultrapure water for 5 times by ultrasound, respectively. Then, three bilayers of PEI/PAA were decorated on SPCE via layer by layer self-assembly to modulate the morphology of gold nanostructures in electrochemical deposition. To obtain ideal gold nanostructures, deposition parameters of gold nanostructures were subsequently investigated. The optimal deposition parameters are as follows: applied potentials (-0.3 V), $4.0 \text{ mg} \cdot \text{mL}^{-1}$ HAuCl_4 and deposition time of 15 min. After electrodeposition of gold nanostructures, the Hp1-contained Tris-HCl buffer (100 mM NaCl, 1.0 mM TCEP, pH 7.4) was prepared and incubated for 30 min in dark. Then, the surfaces of the modified SPCEs were dropped with 6 μL of Hp1 solution with a series of the required concentration for Hp1 self-assembly overnight at room temperature. Subsequently, the SPCEs after Hp1 self-assembly were thoroughly rinsed with 20 mM Tris-HCl buffer (100 mM NaCl, pH 7.4) and dried with nitrogen gas. Finally, the unoccupied region of SPCEs assembled with Hp1 was filled by immersing it into 2 mM MCH solution for 1 h to inhibit the nonspecific DNA adsorption. The modified SPCEs are named as MCH/Hp1/gold/SPCEs.

Detection of CA125

Prior to CA125 detection, MCH/Hp1/gold/SPCEs were rinsed with 20 mM Tris-HCl buffer (100 mM NaCl, pH 7.4) and dried. And aptamer/probe A duplex was formed via hybridization of probe A and CA125 aptamer. Then, CA125 aptamer/probe A duplex (20 μL), Hp2 (20 μL) and various concentrations of CA125 (10 μL) were incubated at 37 $^{\circ}\text{C}$ for 20 min. Subsequently, 6 μL of incubated mixture was dropped on the MCH/Hp1/gold/SPCEs. The hybridization reaction was conducted for 20 min at 37 $^{\circ}\text{C}$ and constant humidity in a hybridization oven (UVP, HB-1000). After that, the MCH/Hp1/gold/SPCEs after hybridization were washed with buffer for measurements. SWV measurements were performed by scanning the potential from -0.5 to -0.1 V in 20 mM Tris-HCl buffer (100 mM NaCl, pH 7.4) with a step potential of 1 mV, a frequency of 60 Hz, and an amplitude of 50 mV.

Results and discussion

Choice of materials

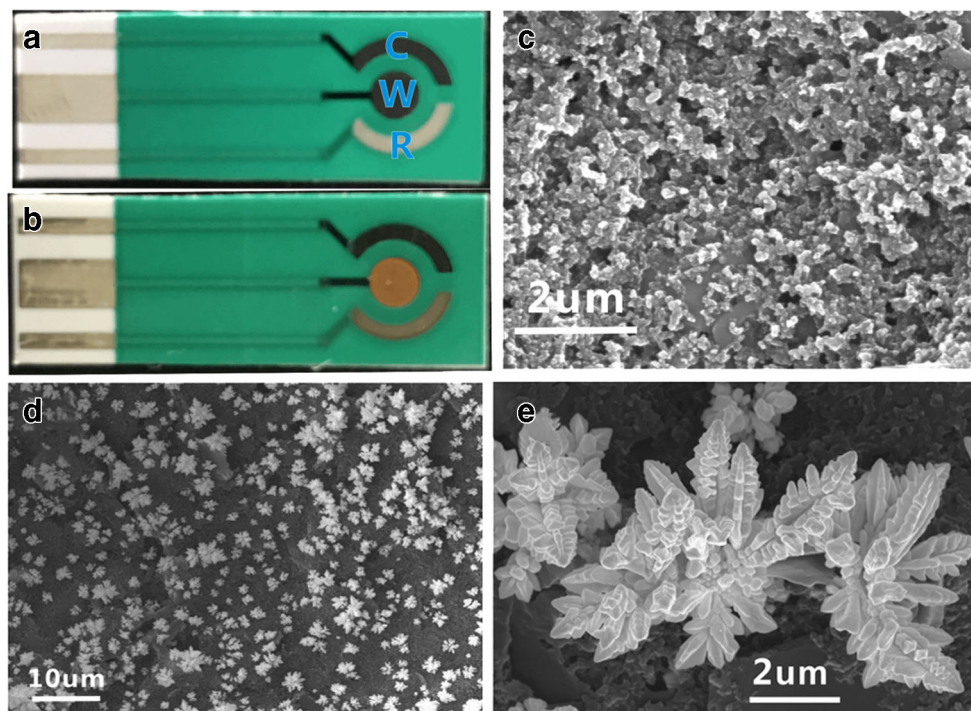
Binding performance of biomolecules on the sensing surface is influenced by surface characteristics [31]. Various nanomaterials such as C-dots [32], molybdenum disulfide (MoS₂) [6, 33], gold nanostructures [34] and et al., are widely used to construct electrochemical biosensors to improve the sensing performance. Among them, gold nanostructures

possess high electrical/thermal conductivities, easy functionalization and large surface areas. More importantly, the performance of gold nanostructures can be easily modified by its size and morphology [35]. Various gold nanostructures including spherical, fractal, and flower-like nanostructures directly programmed on SPCEs by Ye and his co-workers. They found that flower-like nanostructure has the largest surface areas, the highest electrochemical response and favorable reproducibility in DNA probe assembly [34]. Thus, we select flower-like gold nanostructure to be electrodeposited on SPCEs to construct subsequently aptasensing platform of CA 125.

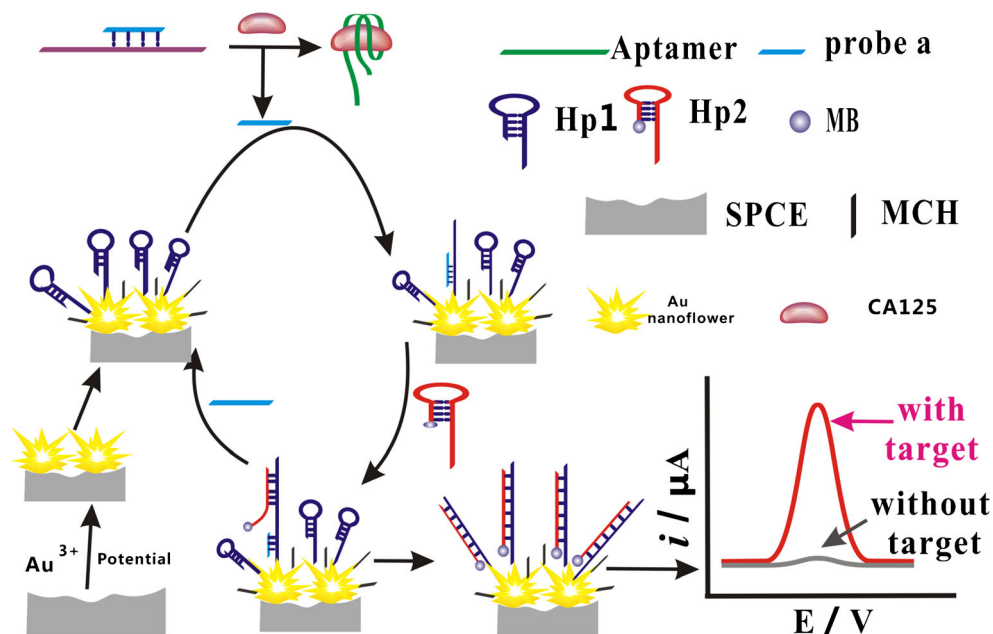
Characterization of construction of aptasensing platform

Flower-like gold nanostructures were electrodeposited on SPCEs with naturally nanoroughened carbon surface (Fig. 1a, c), to construct subsequently aptasensing platform of CA125. The modulation of the morphology of gold nanostructures was discussed in [Electronic Supporting Material](#). By controlling appropriate conditions (deposition potential: -0.3 V, HAuCl₄ concentration: $4 \text{ mg}\cdot\text{mL}^{-1}$, deposition time: 15 min), the flower-like gold nanostructures were successfully generated on the SPCEs surfaces (Fig. 1b, d). As shown in higher-magnification SEM image (Fig. 1e), obvious flower-like morphologies are observed. The introduction of flower-like gold nanostructures can efficiently increase the biosensing surface for assembly of more amounts of probe molecules

Fig. 1 The macro schematic diagrams of the SPCE (a) and the SPCE modified with gold nanostructures (b); C: counter electrode; W: working electrode; R: silver pseudo reference electrode. The SEM images of the surface of SPCE (c) and the surface of SPCE modified with gold nanostructures (d). The higher-magnification SEM image of the surface of SPCE modified with gold nanostructures (e)



Scheme 1 The schematic of electrochemical aptasensing platform of CA-125 and its signal amplification processes.



and subsequent accessibility of target molecules, thus, contributing to higher electrochemical response and more reliable reproducibility for DNA probe assembly in electrochemical biosensing platforms. Corresponding construction processes of aptasensing platform were also characterized by electrochemical impedance spectroscopy (EIS) and cyclic voltammetry (CV). Results and discussion are shown in [Electronic Supporting Material](#).

Principle of the electrochemical CA125 assay

The schematic of electrochemical aptasensing platform of CA125 and its signal amplification is illustrated in Scheme 1. Firstly, the toehold-containing hairpin probes (Hp1 labeled with 5'-SH, Hp2 labeled with MB at 3' end), CA125 aptamer and probe A were synthesized. Then, Hp1 was self-assembled on the surfaces of SPCEs electrodeposited the flower-like gold nanostructures by Au-S bond. Subsequently, to inhibit the nonspecific DNA adsorption, MCH was used for passivating the unoccupied region of the SPCEs surfaces [30]. In this design, the flower-like gold nanostructures can increase biosensing surface and molecular deflection angles, which is benefit for assembly of more amounts of Hp1 and subsequent accessibility of target molecules, respectively. Prior to sensing of CA125, the probe A is hybridized with CA125 aptamer to form aptamer/probe A duplex. In the presence of CA125, CA125 binds to its aptamer because of the specific high binding capacity between CA125 and its aptamer, and probe A is released from aptamer/probe A duplex. The released probe A further hybridizes with toehold of Hp1

to open its hairpin structure. In the presence of MB-labeled Hp2, the toehold domain of Hp2 subsequently hybridizes with the exposed complementary single strands of Hp1 to bring electro-active reporter MB in proximity to the modified SPCEs surface. The probe A is released from probe A-Hp1 duplex and triggers another round strand displacement reaction (SDR). Such a 1:N target-signal DNA recycling amplification leads to plenty of MB in proximity to the surfaces of modified SPCEs and significantly increases the current response.

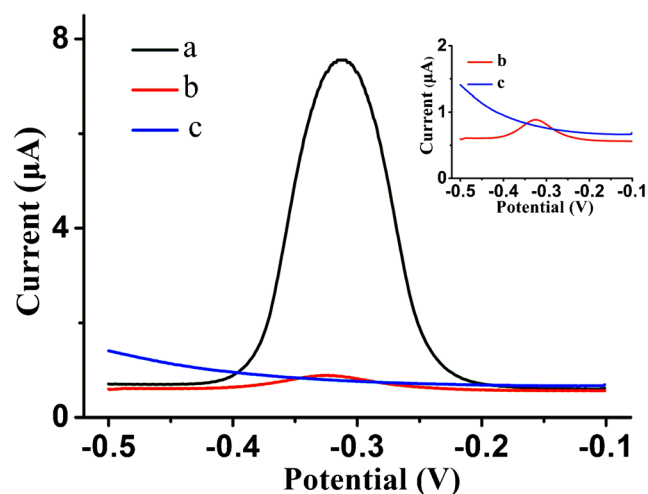


Fig. 2 Typical SWV current responses of (a) SPCE modified with AuNSs incubated with CA125 aptamer/probe A and Hp2 in the presence of CA125 ($1.0 \text{ ng}\cdot\text{mL}^{-1}$); (b) SPCE modified with AuNSs incubated with CA125 aptamer/probe A and Hp2 without CA125; (c) SPCE modified with AuNSs

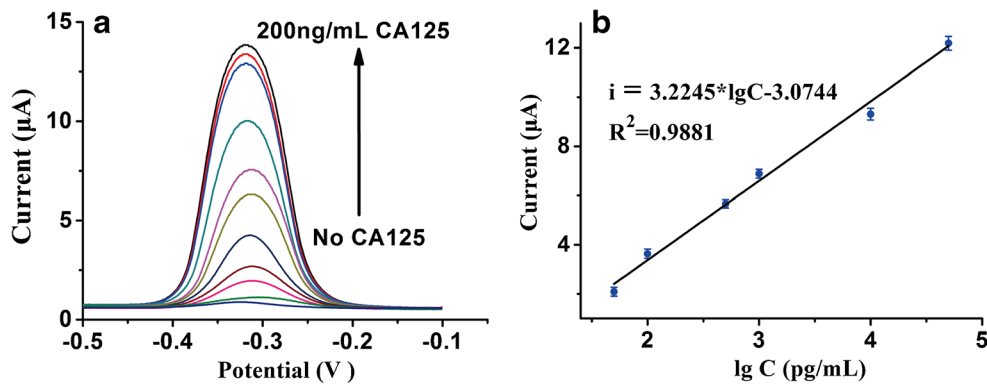


Fig. 3 **a** Typical SWV current responses of the SPCE modified with AuNSs to a series of CA125 concentration, from bottom to top: 0.5 pg·mL⁻¹, 10 pg·mL⁻¹, 50 pg·mL⁻¹, 100 pg·mL⁻¹, 500 pg·mL⁻¹, 1 ng·mL⁻¹, 10 ng·mL⁻¹, 50 ng·mL⁻¹,

100 ng·mL⁻¹, and 200 ng·mL⁻¹. **b** The calibration plot between SWV current and the logarithm of the concentration of CA125. The data were acquired at -0.313 v to establish calibration plot. Error bars: SD, $n = 3$

Feasibility of the method

To further verify the feasibility of the electrochemical aptasensing platform of CA-125, SWV measurements were performed in 20 Mm Tris-HCl buffer (0.1 M NaCl, pH 7.4) containing different complexes. As shown in Fig. 2, no peak current is observed in the absence of CA125 aptamer/probe A, Hp2 and CA125 because of no electro-active reporter MB on the modified SPCEs surface (curve c). When the modified SPCE is incubated with CA125 aptamer/probe A and Hp2 without CA125, negligible current changes can be seen (curve b), in that the inhibition of SDR triggered by probe A, in the absence of CA125, brings no MB in proximity to the modified SPCEs surface. However, when the modified SPCE is incubated with CA125 aptamer/probe A and Hp2 in the presence of CA125 (1.0 ng·mL⁻¹), a significant peak current is observed

(curve a). Such a significant current increase implies plenty of MB in proximity to the surfaces of modified SPCEs, owing to the occurrence of CA125 triggered probe A recycling amplification. These results clearly demonstrate the feasibility of the electrochemical aptasensing platform of CA-125.

Optimization of the assay conditions

To achieve the optimal performance of electrochemical aptasensing platform, several experimental parameters were optimized, including the concentration of Hp1, the concentration of CA125 aptamer, pH and the reaction time. The optimal reaction conditions are as follows: the concentration of Hp1 (2.0 µM); the concentration of CA125 aptamer (40 nM); pH (7.4); the reaction time (20 min). The corresponding data and figures are presented in [Electronic Supporting Material](#).

Table 1 Comparison of our method with reported electrochemical sensors for detection of CA125

Type of sensor	Detection method	LOD	Dynamic range	References
Immunosensor based on FA, H-PANI and CS-HCl	SWV	0.25 pg·mL ⁻¹	0.001–25 ng·mL ⁻¹	5
Biosensor platform based on multiwalled carbon nanotubes embedded zinc oxide nanowire	DPV	0.00113 U·mL ⁻¹	0.001–1000 U·mL ⁻¹	13
Immunosensor based on ZnO nanorods-Au nanoparticles nanohybrids	CV	2.5 ng·µL ⁻¹	–	14
Immunosensor based on covalent immobilization of CA125 coupled with thionine on carbon nanofiber	DPV	1.8 U·mL ⁻¹	2–75 U·mL ⁻¹	15
Engineered MPA AuNP@SiO ₂ QD mAb immunosensor	EIS	0.0016 U·mL ⁻¹	0–0.1 U·mL ⁻¹	16
Immunosensor based on polyaniline-polythionine redox hydrogel	SWV	0.00125 U·mL ⁻¹	0.0001–1000 U·mL ⁻¹	17
Immunosensor using GOx label-based EN redox cycling	CA	0.15 U·mL ⁻¹	–	18
Sensor based on protein imprinted polymer on GNEE	DPV	0.5 U·mL ⁻¹	0.5–400 U·mL ⁻¹	19
Electrochemical aptasensing platform based on combination of target-triggered SDA and aptamer recognition	SWV	5.0 pg·mL ⁻¹	0.05–50 ng·mL ⁻¹	This work

DPV differential pulse voltammetry; CV cyclic voltammetric; EIS electrochemical impedance spectroscopy; SWV square wave voltammetry; CA chronoamperometry; GNEE gold nanoelectrode ensemble; FA ferrocenecarboxylic acid; H-PANI HCl-doped polyaniline; CS-HCl chitosan hydrochloride

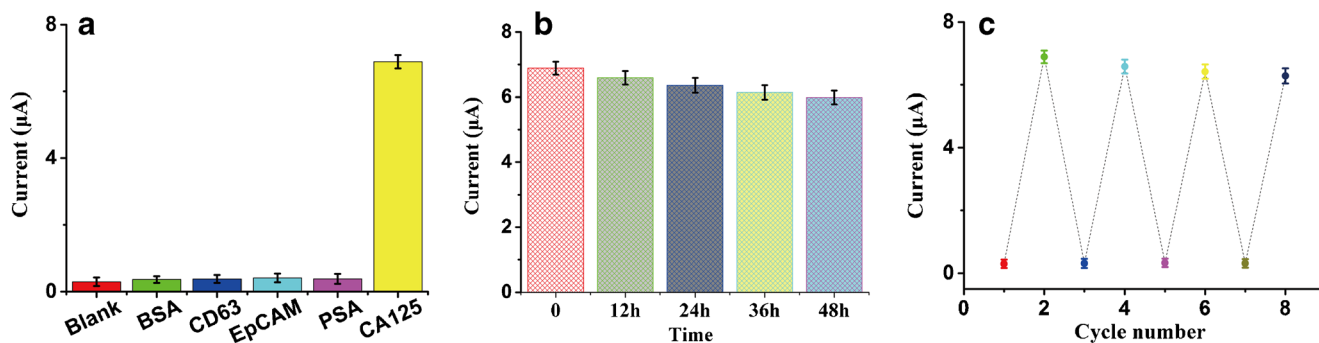


Fig. 4 Specificity (a), stability (b) and regeneration (c) of the aptasensing platform of CA125. Error bar: SD, $n = 3$

Analytical performance of the method

The sensitivity and dynamic response range are important indicators for evaluating analytical performance of the sensor. Under the optimal sensing conditions, using a series of CA125 concentrations ranging from 0 to 200 $\text{ng}\cdot\text{mL}^{-1}$, we investigated the performance of this aptasensing platform. We can clearly see that the current response gradually increases along with increasing of CA125 concentration (Fig. 3a). Besides, the SWV current is logarithmically related to the concentration of CA125 from 0.05 to 50 $\text{ng}\cdot\text{mL}^{-1}$. We calculated the regression equation expressed as $i = 3.2245\lg C - 3.0744$ ($R^2 = 0.9881$), where i stands for the SWV current and C stands for the concentration of CA125 (Fig. 3b). The detection limit calculated is as low as $0.005 \text{ ng}\cdot\text{mL}^{-1}$, which is comparable or even lower to the reported methods (listed in Table 1).

Specificity, stability and regeneration

The specificity of the aptasensing platform of CA125 relies on the specific recognition of aptamer to CA125. The specificity was assessed by detecting different proteins,

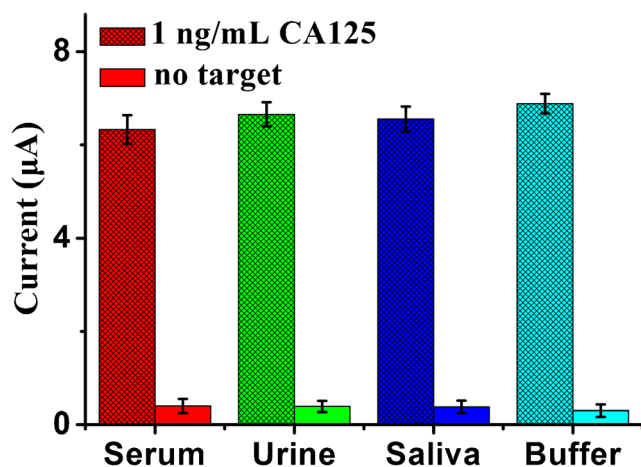


Fig. 5 The SWV currents of electrochemical aptasensing platform for detecting CA125 in several spiked biological samples, such as serum, urine and saliva. Error bar: SD, $n = 3$

such as BSA ($10 \text{ ng}\cdot\text{mL}^{-1}$), CD63 ($10 \text{ ng}\cdot\text{mL}^{-1}$), EpCAM ($10 \text{ ng}\cdot\text{mL}^{-1}$) and PSA ($10 \text{ ng}\cdot\text{mL}^{-1}$). Negligible current increase of above proteins are observed when compared with blank, which are far less than that of CA125 ($1.0 \text{ ng}\cdot\text{mL}^{-1}$) (Fig. 4a). The results demonstrate the good specificity of the aptasensing platform of CA125. The stability of this biosensor was investigated by detecting CA125 ($1.0 \text{ ng}\cdot\text{mL}^{-1}$) at different time points within 48 h after storage at $4 \text{ }^\circ\text{C}$. Compared with initial current signal, only a small current decrease is observed (Fig. 4b), indicating the excellent stability of the aptasensing platform of CA125. Moreover, the regeneration experiment of the sensor was also performed by rinsing the sensor in 5 M urea for 10 min at $37 \text{ }^\circ\text{C}$. After five regeneration cycles, the current response is almost still at its first current signal level, indicating satisfied regeneration of the sensor (Fig. 4c).

Analysis of biological samples

The practical application potential of the sensor in clinical was evaluated by detecting CA125 in the spiked serum, urine and saliva. MCH/HP1/gold/SPCEs were rinsed with 20 mM Tris-HCl buffer (100 mM NaCl, pH 7.4) and dried. And aptamer/probe A duplex was formed via hybridization of probe A and CA125 aptamer. For preparation of the spiked samples, 20 μL different biological samples were diluted by 180 μL 20 mM Tris-HCl buffer (100 mM NaCl, pH 7.4) and CA125 were spiked, with concentration of $1.0 \text{ ng}\cdot\text{mL}^{-1}$. The subsequent detection processes follow the section of "Detection of CA125". The SWV current changes at -0.313 V were acquired. As shown in Fig. 5, significant current increases are observed in above spiked biological samples when compared with no spiked biological samples. In addition, the increased current signals in different spiked biological samples are comparable to that of the spiked buffer, with the recoveries between 82.5% and 104.1% (Table S2). These results implies good selectivity and a potential practicability in clinical.

Conclusion

An electrochemical aptasensing platform was designed to detect CA125, which was based on the basis of combination of aptamer recognition and target-triggered SDA. It was successfully applied to detect CA125 in spiked biological samples. However, we only detected CA125 in the spiked samples which were diluted by buffer, due to the complex matrix components in clinical samples. Encouragingly, our method may combine with microfluidic chip which has the better separation performance, showing a good application prospect for analysis of clinical samples. In addition, this method may be expanded to detect other molecules by selecting corresponding aptamers.

Acknowledgements These works were supported by the National Natural Science Foundation of China (81872509), the Hubei Provincial Technology Innovation Project (2017ACA176), the Free Exploration Project of Hubei University of Medicine (FDFR201804), the Key Discipline Project of Hubei University of Medicine and the Foundation of Health Commission of Hubei Province (WJ2019M054), the Research Project of Traditional Chinese Medicine of the Foundation of Health Commission of Hubei Province (ZY2019M034), the Open Project of Hubei Key Laboratory of Wudang Local Chinese Medicine Research (Hubei University of Medicine)(WDCM2018004), the Science and Technology Key Program of Shiyan (No.18Y101, 18Y102 and 18Y104).

Compliance with ethical standards The author(s) declare that they have no competing interests.

References

- Zhao T, Hu W (2016) CA125 and HE4: measurement tools for ovarian Cancer. *Gynecol Obstet Inves* 81(5):430–435
- Yang ZJ, Zhao BB, Li L (2016) The significance of the change pattern of serum CA125 level for judging prognosis and diagnosing recurrences of epithelial ovarian cancer. *J Ovarian Res* 9(1):57
- Felder M, Kapur A, Gonzalez-Bosquet J, Horibata S, Heintz J, Albrecht R, Fass L, Kaur J, Hu K, Shojaei H (2014) MUC16 (CA125): tumor biomarker to cancer therapy, a work in progress. *Mol Cancer* 13(1):129
- Zhang K, Shen X (2013) Cancer antigen 125 detection using the plasmon resonance scattering properties of gold nanorods. *Analyst* 138(6):1828–1834
- Ren X, Wang H, Wu D, Fan D, Zhang Y, Du B, Wei Q (2015) Ultrasensitive immunoassay for CA125 detection using acid site compound as signal and enhancer. *Talanta* 144:535–541
- Ding C, Song K, Meng H, Zhang B, Zhao Z, Chang H, Wei W (2018) Amplified photoelectrochemical immunoassay for the tumor marker carbohydrate antigen 724 based on dye sensitization of the semiconductor composite C3N4-MoS2. *Microchim Acta* 185(12):530
- Nie Y, Yang M, Ding Y (2018) Gold nanoparticle enhanced hybridization chain reaction as a method for signal amplification. Application to electrochemical immunodetection of the ovarian cancer biomarker carbohydrate antigen 125. *Microchim Acta* 185(7):331
- Samadi Pakchin P, Ghanbari H, Saber R, Omid Y (2018) Electrochemical immunosensor based on chitosan-gold nanoparticle/carbon nanotube as a platform and lactate oxidase as a label for detection of CA125 oncomarker. *Biosens Bioelectron* 122:68–74
- Jin H, Gui R, Gong J, Huang W (2017) Aptamer and 5-fluorouracil dual-loading Ag2S quantum dots used as a sensitive label-free probe for near-infrared photoluminescence turn-on detection of CA125 antigen. *Biosens Bioelectron* 92:378–384
- Mansouri Majd S, Salimi A (2018) Ultrasensitive flexible FET-type aptasensor for CA 125 cancer marker detection based on carboxylated multiwalled carbon nanotubes immobilized onto reduced graphene oxide film. *Anal Chim Acta* 1000:273–282
- Lamberti I, Scarano S, Esposito CL, Antocchia A, Antonini G, Tanzarella C, Francis VD, Minunni M (2016) In vitro selection of RNA aptamers against CA125 tumor marker in ovarian cancer and its study by optical biosensing. *Methods* 97:58–68
- Hamd-Ghadareh S, Salimi A, Fathi F, Bahrami S (2017) An amplified comparative fluorescence resonance energy transfer immunosensing of CA125 tumor marker and ovarian cancer cells using green and economic carbon dots for bio-applications in labeling, imaging and sensing. *Biosens Bioelectron* 96:308–316
- Paul KB, Singh V, Vanjari SRK, Singh SG (2017) One step biofunctionalized electrospun multiwalled carbon nanotubes embedded zinc oxide nanowire interface for highly sensitive detection of carcinoma antigen-125. *Biosens Bioelectron* 88:144–152
- Gasparotto G, Costa JPC, Costa PI, Zaghet MA, Mazon T (2017) Electrochemical immunosensor based on ZnO nanorods-au nanoparticles nanohybrids for ovarian cancer antigen CA-125 detection. *Mat Sci Eng C-Mater* 76:1240–1247
- Wu L, Yan F, Ju H (2007) An amperometric immunosensor for separation-free immunoassay of CA125 based on its covalent immobilization coupled with thionine on carbon nanofiber. *J Immunol Methods* 322(1–2):12–19
- Johari-Ahar M, Rashidi MR, Barar J, Aghaie M, Mohammadnejad D, Ramazani A, Karami P, Coukos G, Omid Y (2015) An ultrasensitive impedimetric immunosensor for detection of the serum oncomarker CA-125 in ovarian cancer patients. *Nanoscale* 7(8): 3768–3779
- Zhao L, Ma Z (2018) Facile synthesis of polyaniline-polythionine redox hydrogel: conductive, antifouling and enzyme-linked material for ultrasensitive label-free amperometric immunosensor toward carcinoma antigen-125. *Anal Chim Acta* 997:60–66
- Singh A, Park S, Yang H (2013) Glucose-oxidase label-based redox cycling for an incubation period-free electrochemical immunosensor. *Anal Chem* 85(10):4863–4868
- Viswanathan S, Rani C, Ribeiro S, Delerue-Matos C (2012) Molecular imprinted nanoelectrodes for ultra sensitive detection of ovarian cancer marker. *Biosens Bioelectron* 33(1):179–183
- Al-Ogaidi I, Gou H, Aguilar ZP, Guo S, Melconian AK, Al-Kazaz AK, Meng F, Wu N (2014) Detection of the ovarian cancer biomarker CA-125 using chemiluminescence resonance energy transfer to graphene quantum dots. *Chem Commun* 50(11):1344–1346
- Wang G, Jin F, Dai N, Zhong Z, Qing Y, Li M, Yuan R, Wang D (2012) Signal-enhanced electrochemiluminescence immunosensor based on synergistic catalysis of nicotinamide adenine dinucleotide hydride and silver nanoparticles. *Anal Biochem* 422(1):7–13
- Zhao L, Han H, Ma Z (2018) Improved screen-printed carbon electrode for multiplexed label-free amperometric immunosensor: addressing its conductivity and reproducibility challenges. *Biosens Bioelectron* 101:304–310
- Zou Y, Liang J, She Z, Kraatz HB (2019) Gold nanoparticles-based multifunctional nanoconjugates for highly sensitive and enzyme-free detection of E.coli K12. *Talanta* 193:15–22
- Nunna BB, Mandal D, Lee JU, Singh H, Zhuang S, Misra D, Bhuyian MNU, Lee ES (2019) Detection of cancer antigens (CA-125) using gold nano particles on interdigitated electrode-based microfluidic biosensor. *Nano convergence* 6(1):3

25. Hasanzadeh M, Sahmani R, Solhi E, Mokhtarzadeh A, Shadjou N, Mahboob S (2018) Ultrasensitive immunoassay of carcinoma antigen 125 in untreated human plasma samples using gold nanoparticles with flower like morphology: a new platform in early stage diagnosis of ovarian cancer and efficient management. *Int J Biol Macromol* 119:913–925
26. Huang Z, Luo Z, Chen J, Xu Y, Duan Y (2018) A facile, label-free and universal biosensor platform based on target-induced graphene oxide constrained DNA dissociation coupling with improved Strand displacement amplification. *ACS sensors* 26:2423–2431. <https://doi.org/10.1021/acssensors.8b00935>
27. Liu H, Luo J, Fang L, Huang H, Deng J, Huang J, Zhang S, Li Y, Zheng J (2018) An electrochemical strategy with tetrahedron rolling circle amplification for ultrasensitive detection of DNA methylation. *Biosens Bioelectron* 121:47–53
28. Wei X, Duan X, Zhou X, Wu J, Xu H, Min X, Ding S (2018) A highly sensitive SPRi biosensing strategy for simultaneous detection of multiplex miRNAs based on strand displacement amplification and AuNP signal enhancement. *Analyst* 143(13):3134–3140
29. Tian L, Qi J, Ma X, Wang X, Yao C, Song W, Wang Y (2018) A facile DNA strand displacement reaction sensing strategy of electrochemical biosensor based on N-carboxymethyl chitosan/molybdenum carbide nanocomposite for microRNA-21 detection. *Biosens Bioelectron* 122:43–50
30. Chen Q, Hu W, Shang B, Wei J, Chen L, Guo X, Ran F, Chen W, Ding X, Xu Y, Wu Y (2018) Ultrasensitive amperometric aptasensor for the epithelial cell adhesion molecule by using target-driven toehold-mediated DNA recycling amplification. *Microchim Acta* 185(3):202
31. Buk V, Pemble ME, Twomey K (2019) Fabrication and evaluation of a carbon quantum dot/gold nanoparticle nanohybrid material integrated onto planar micro gold electrodes for potential bioelectrochemical sensing applications. *Electrochim Acta* 293: 307–317
32. Shu Z, Xia L, Ran P, Mo F, Qiao X, Fu Y (2017) A glassy carbon electrode modified with C-dots and silver nanoparticles for enzymatic electrochemiluminescent detection of glutamate enantiomers. *Microchim Acta* 184(12):4679–4684
33. Soni A, Pandey CM, Pandey MK, Sumana G (2019) Highly efficient polyaniline-MoS₂ hybrid nanostructures based biosensor for cancer biomarker detection. *Anal Chim Acta* 1055:26–35
34. Ye L, Yang F, Ding Y, Yu H, Yuan L, Dai Q, Sun Y, Wu X, Xiang Y, Zhang G-J (2018) Bioinspired trans-scale functional interface for enhanced enzymatic dynamics and ultrasensitive detection of microRNA. *Adv Funct Mater* 28(17):1706981
35. Su S, Wu Y, Zhu D, Chao J, Liu X, Wan Y, Su Y, Zuo X, Fan C, Wang L (2016) On-electrode synthesis of shape-controlled hierarchical flower-like gold nanostructures for efficient interfacial DNA assembly and sensitive electrochemical sensing of MicroRNA. *Small* 12(28):3794–3801

Publisher's note Springer Nature remains neutral with regard to jurisdictional claims in published maps and institutional affiliations.